Published in final edited form as:
Nat Neurosci. 2014 October ; 17(10): 1313–1315. doi:10.1038/nn.3768.

"Silent" mitral cells dominate odor responses in the olfactory bulb of awake mice

Mihaly Kollo[1,2,*], **Anja Schmaltz**[1,2], **Mostafa Abdelhamid**[1,3], **Izumi Fukunaga**[1,2], and **Andreas T Schaefer**[1,2,3,4,*]

[1]Behavioural Neurophysiology, Max-Planck-Institute for Medical Research, Heidelberg, Germany

[2]Division of Neurophysiology, MRC National Institute for Medical Research, London, UK

[3]Dept. Anatomy & Cell Biology, Faculty of Medicine, University of Heidelberg, Germany

[4]Dept. of Neuroscience, Physiology & Pharmacology, University College London, UK

Abstract

How wakefulness shapes neural activity is a topic of intense discussion; in the awake olfactory bulb, high activity with weak sensory-evoked responses were reported in mitral/tufted cells (M/TCs). Using blind whole-cell recordings, we find 33% of M/TCs to be "silent", yet showing strong sensory responses - with weak or inhibitory responses in "active" neurons. Thus, a previously missed M/TC subpopulation can exert powerful influence over the olfactory bulb.

Sensory processing is thought to be profoundly influenced by behavioral state. Substantial amounts of data have been obtained from anesthetized preparations, yet recent results from awake animals suggest significantly altered network activity[1–5]. In the olfactory system, studies using extracellular local field potential and single unit recordings[3–9] or calcium imaging [2,10,11] report substantially increased baseline activity of M/TCs in the awake animal (but see [3]) and only weak, transient, or inhibitory odor-evoked responses (but see [12]). All currently available techniques, however, allow recording from only a fraction of neurons in mammalian neuronal networks[13]. Therefore the sampling characteristics and internal error sources of different recording techniques have to be taken into consideration to gain global insight into network dynamics[14,15].

We have used blind whole-cell recordings to measure the activity *in vivo* of 125 olfactory bulb neurons in the awake, alert (Supplementary Figs. 1 and 2) and 179 neurons in the anesthetized state. Recordings from M/TCs revealed highly heterogeneous baseline states (Fig. 1). The resting membrane potentials of M/TCs showed significantly larger dispersion

*Correspondence: andreas.schaefer@mpimf-heidelberg.mpg.de. *Correspondence: mihaly.kollo@mpimf-heidelberg.mpg.de.

CONTRIBUTIONS: M.K. and A.T.S. designed and conceived all experiments; A.S. designed the headplate and the treadmill. M.K. performed the awake recordings and the computational analyses, M.K. and I.F carried out the anesthetized experiments. M.A. performed the behavioral experiments. M.K. and A.T.S. analyzed and interpreted the data and modeling results. M.K. and A.T.S. wrote the article with contributions from all authors.

COMPETING FINANCIAL INTERESTS: The authors declare no competing financial interests.

Europe PMC Funders Author Manuscripts

in awake animals (Fig. 1c,f,g; p=0.020, modified robust Brown-Forsythe Levene test; IQR_{AWAKE}=6.32 mV, $IQR_{ANESTHETIZED}$=4.83 mV), with more neurons at relatively hyperpolarized or relatively depolarized membrane potentials (Fig. 1g). Consequently, in awake animals a larger proportion of cells were highly active (firing rate > 10Hz in 15% of M/TCs vs. 5% in anesthetized, Fig. 1h), yet both in the awake and anesthetized state one third of the neurons showed very low baseline firing rates (<0.1Hz). Thus, consistent with previous studies[3,8,12] we find that under baseline conditions there are substantially more highly active cells in the awake than in the anesthetized preparation. Blind whole-cell recordings, however, additionally uncover a substantial "silent" subpopulation of M/TCs that rarely or never spontaneously discharge action potentials in the awake animal but are otherwise indistinguishable from more "active" cells (Supplementary Fig. 2).

We next characterized the evoked response profiles of neurons to short (1–2.5 s) odor pulses presented passively to the animals or during an odor discrimination task (Supplementary Fig. 1). Activity of M/TCs was modulated in a highly diverse manner by odor stimulation in awake mice: The occurrence of inhibitory and excitatory responses was balanced (54% excitatory, 46% inhibitory, Fig. 2b), however in some neurons we observed particularly strong phasic depolarizing reactions to odorants (Fig. 2a, bottom). Remarkably, it were M/TCs with low spontaneous firing activity that responded predominantly with depolarization and increased firing rate, while M/TCs with high baseline spiking activity (in agreement with previous observations[3,8]), responded mostly with weak excitation or hyperpolarization (Fig. 2c; p = 0.000016, MW-U test; n = 52 and 50 significant odor responses; Supplementary Fig. 6). Similarly, response profiles of more depolarized cells showed a preference for inhibitory or only weakly excitatory responses (Fig. 2d; $\rho = -0.39$, $p < 0.00001$, Spearman's rank correlation), while hyperpolarized cells regularly responded to odorants with strong, phasic depolarization. A weaker, but similar relationship was found under anesthesia (Supplementary Figs. 3, 6). Conversely, in control trials without odors, no significant correlation was found between recent membrane potential and response ($\rho = -0.0084$, p=0.87) or recent firing rate and response ($\rho = -0.027$, p=0.61), confirming that the association in odor trials does not arise from regression to mean that could derive from e.g. random fluctuations in the baseline of M/TCs.

Most unit recordings report an overall increase in baseline activity [4,8,12] (but see[3]) and weaker excitatory responses in awake compared to anesthetized preparations[3,8] (but see[12]), that we similarly observed in the more active cells measured with whole-cell recordings (Supplementary Table). Also, multiple studies reported transient[3–5] as well as context-dependent responses[7,16,17] in M/TCs. We intriguingly found that the gross time courses of responses somewhat differ between anesthetized and awake state. Phasic responses during odor presentation were closely matched between awake and anesthetized state (Fig 2, Supplementary Fig. 6). Long-lasting responses that well exceeded the time of odor presentation[18], however, were much more common in the anesthetized state (Supplementary Fig. 7, see also [11]).

Thus, here we found that - contrary to what has been suggested previously - the transition from the anesthetized to the awake state is not characterized by an overall increase in activity and a reduction of responses to primary sensory stimuli. Instead, the variability of

M/TC activity is increased. This in turn creates a population of highly active, weakly odor-responding cells; there is, however, a continuum of firing rates including a substantial population of cells in the awake that is virtually silent at baseline conditions but can vigorously respond to odor presentation. While whole-cell recordings themselves might suffer from specific biases and technical drawbacks they can record from cells that show little or no spiking under resting conditions – a population of cells that has not been studied intensely with recording techniques predominantly relying on action potentials for cell identification. An intriguing aspect of the observed heterogeneity in both the baseline activity levels and odor responses of M/TCs is how the divergent principal cells might influence postsynaptic local interneurons (INs), and consequently the transformation of odor representations in the olfactory bulb, including proposed circuit functions such as contrast enhancement or pattern completion. Our results indicate that M/TCs with high baseline firing rates would be less able to exert a strong excitatory effect onto and thus recruit INs: Firstly, these neurons rarely respond with depolarization to odorants, which would be necessary to evoke increased transmitter release. Moreover, excitatory synapses between M/TCs and INs express short-term depression[19,20]. Consequently, synapses from highly active M/TCs will be depressed compared to synapses from low firing rate M/TCs (Supplementary Figs. 4 and 8). Downstream targets, in turn, might be engaged preferentially by different populations of M/TCs through largely facilitating synapses. Mechanistically, differing electrical driving force, feedback within the glomerulus or onto olfactory sensory neuron terminals might contribute to the activity-dependence of evoked responses. Recordings in behaving, awake animals indicated that M/TCs activity is highly dynamic at longer time scales[2] and is influenced by inputs from higher order brain regions[7,9], suggesting that the principal source of variability of neuronal activity in the MOB in awake animals is strong top-down modulation. It remains to be shown how the different behavioral states may influence the pattern of M/TC baseline activity.

ONLINE METHODS

Animals

C57BL/6J mice aged 4–7 weeks were used in both anesthetized and awake recordings. Animals from both sexes were used randomly (49.5%/50.5%). Before experiments, up to 5 animals were co-housed in a cage, from the start of the experiment, animals were housed in separate cages. Animals were kept in normal light/dark cycle, behavioural experiments were performed during the night hours.. All animal experiments were performed in accordance with the German Animal Welfare Act.

Surgery

Mice were anesthetized using ketamine (100 mg/kg) and xylazine (20 mg/kg for induction, 10 mg/kg for maintenance) administered intraperitoneally and supplemented as required. Body temperature was maintained at 37.0 °C with a feedback-regulated heating pad (FHC, Bowdoin, ME, USA). A custom made steel or PEEK headplate was fixed to the parietal bone plates with cyanoacrylate and dental cement. During surgery, meloxicam (2.5 mg/kg) was injected intraperitoneally for post-operative analgesia. Animals were allowed to recover for 2-7 days. On the day of the recording, under brief isoflurane anesthesia (1.5%, analgesia

was provided by 2.5 mg/kg IP meloxicam and local application of 1% lidocain), a small (0.4-0.8 mm) craniotomy was drilled above the olfactory bulb. For anesthetized recordings, ketamine and xylazine was administered intraperitoneally. After removal of the dura, the craniotomy was covered by a layer of low-melting point agarose (0.5-1 mm). The chamber surrounding the craniotomy was filled with Ringer solution (135 mM NaCl, 5.4 mM KCl, 5 mM HEPES, 1 mM MgCl2, 1.8 mM $CaCl_2$, pH 7.2, 285 mOsm/kg) to prevent desiccation. For awake recordings, animals were head-fixed on a linear treadmill as described before[21] to minimize stress. Following awakening after surgery, the animals were allowed to recover for at least 30 minutes before electrophysiological recordings commenced[22]. No overt stress responses were observed and all animals readily accepted food and licked for rewards well before that time. Consistent with previous studies[2] no differences were found if animals were acclimatized to the head-fixation over the course of several days (e.g. Supplementary Figs. 1, 6) and data was thus pooled.

Odor delivery

Odors (anisaldehyde, cinnamaldehyde, cyclohexanol, estragol, eugenol, isoamyl acetate, methyl salycilate, 1-octanol, phenyl-ethanol, salycilate and vanillin) were presented using a custom-made airflow dilution olfactometer with electronic dilution control to result in a final concentration of on average 40 ppm (range 0.1-520 ppm). Odors were presented individually with a minimal inter-trial interval of 10 s. No intrinsic aversive or attractive behavioral reaction to the odors was observed and all odors were readily learned as S+ as well as S− stimuli. To achieve minimal contamination and a reproducible stimulus shape, the olfactometer was washed by a strong stream of clean air between odor trials, while constant air flow to the animal was established by a final valve at the odor port. A photo ionization detector (miniPID, Aurora Scientific, Ontario Canada) was used regularly to determine the time course of odor presentation and ascertain the absence of contamination.

Electrophysiology

Whole-cell recordings were made as described previously[14], with borosilicate glass capillaries pulled to 5–10 MΩ resistance when filled with solution containing (in mM): KMeSO4 (130), HEPES (10), KCl (7), ATP-Na (2), ATP-Mg (2), GTP (0.5), EGTA (0.05), biocytin (10) and Alexa594 (10). pH and osmolality were adjusted to 7.3 and 275–280 mOsm/kg, respectively. Signals were amplified using a Multiclamp 700B amplifier (Molecular Devices, Sunnyvale, CA) and digitized by a Micro 1401 (Cambridge Electronic Design, Cambridge, UK) at 30 kHz. Drift in membrane potential between the first 5 seconds and first one minute was −1.07 ± 2.75 mV (mean ± SD), and 0.78 ± 0.82 mV between the first minute and the first ten minutes. Recording lengths from M/TCs in awake animals ranged from 0.5-35 min, with a median of 11.34 min.

Identification of cell classes

For postmortem morphological identification of neurons (22 of 304 recorded neurons were recovered sufficiently well to allow for unequivocal identification as interneuron or principal neuron [M/TC]), Alexa594-filled cells were imaged using a custom-built two-photon microscope. Subsequently, mice were perfused following the acute electrophysiological experiment with cold PBS (in mM): NaCl (137), KCl (2.8), KH2PO4 (1.5), Na2HPO4 (8.1),

pH7.4, osmolality (286 mOsm/kg) followed by 4% formaldehyde solution in PBS. Fixed OBs were cut with a vibratome (Microm, Walldorf, Germany) and stained with avidin-biotinylated peroxidase (ABC kit, Vector Labs, Burlingame, CA) and the diaminobenzidine reaction. Biocytin stained cells were traced using a Neurolucida system (Micro Bright Field, Williston, VT). Mitral and tufted cells were identified by a cell body located in the mitral cell layer or the external plexiform layer, respectively, the presence of an apical dendrite progressing into the glomerular layer and lateral dendrites branching in the external plexiform layer. In order to separate all M/TC recordings from other cell types, we performed hierarchical clustering of the cells using three factors (Supplementary Fig. 2). The factors were produced by independent component analysis of the after-potential waveform (2 – 25 ms after the peak of the spike) of the average action potential of each cell. The after-potential was used because it is less sensitive to variability in access resistance, and distinctly characteristic to the recorded cell types. The clustering resulted in a clear and complete separation of morphologically identified mitral and tufted cells from other cell types (Supplementary Fig. 2). The activity of the cells showed no correlation to the three factors and accordingly active and inactive cells distributed evenly in the cluster. Notably, neither input resistance, nor other cellular parameters (except resting membrane potential) differed between “silent” and “active cells (Supplementary Fig. 2)

Simulations

The time course of postsynaptic currents in GCs have been estimated in simulation using measured M/TC spike trains and a theoretical model of synaptic depression[23,24]. Granule cell EPSC waveforms were generated by a normalized alpha function,

$$EPSC_0(t) = \alpha \cdot t \cdot \frac{e}{\tau_E} \cdot e^{\frac{-t}{\tau_E}} \quad (1)$$

where τ_E (3.6 ms) is the EPSC decay time constant and a denotes the maximal EPSC amplitude (−40 pA, ref. [25]). During a prolonged spike train, synaptic availability decreases due to synaptic depression. At each spike, the amount of synaptic depression (D) was updated by a linear constant (d).

$$D_0 = 1 \quad (2)$$

$$D\left(t_{sp}^{+}\right) = d \cdot D\left(t_{sp}^{-}\right) \quad (3)$$

Between spikes, D recovered exponentially back toward 1 with first order kinetics with the time constant τ_d:

$$\tau_D \cdot \frac{dD}{dt} = 1 - D \quad (4)$$

The resulting EPSC waveform was calculated as:

$$EPSC_i(t) = D(t_i) \cdot EPSC_0(t - t_i) \quad (5)$$

The simulated current trace for the whole recording was calculated as the linear sum of EPSC waveforms:

$$I(t) = \Sigma_{i=0}^{n} EPSC_i(t) \quad (6)$$

Data Analysis

Odor responses were calculated as activity in the first 1 s from the beginning of odor stimulation in relation to the 1 s preceding the stimulus. Baseline was defined as the period 2 s to 1 s before the odor pulse. For control trials, responses were defined as the last 1 s preceding the stimulus in comparison to the time interval between 2 s and 1 s before the stimulus. Significant odor responses were defined by a bootstrapping method: 100 random 2 sec regions were chosen from the baseline period, and the distribution of membrane potential difference between the first and the second half of the random windows was determined. Sensory responses with absolute membrane potential deviations exceeding the 95th percentile of the baseline fluctuation were considered significant. Voltage traces of M/TCs were normalized for offset related to the median spike threshold (−38.48 mV). Four cells in which external current was injected during the baseline period (before odorant application) were included into the cluster analysis but omitted from the analysis of membrane potential (Fig. 1 c,f,g, Fig 2d; one cell in the anesthetized state, three cells in the awake state). Membrane potential values were not corrected for the liquid junction potential. Data analysis was performed using Spike2 (Cambridge Electronic Design) and R 3.0.1 (R Core Team, 2013; http://www.R-project.org/). Sample sizes used are similar to those reported in the field and no statistical method was used to predetermine these. Animals were randomly chosen from the same age group for awake and anesthetised experiments. Male and female mice were used randomly. Odor stimuli were presented in a random order. Data collection and analysis were not performed blind to the conditions of the experiments. Due to the non-normal distribution of the data, non-parametric hypothesis tests and measures of statistical dependence were used. For comparison of odor responses in active and silent cell populations, homogeneity of variances was tested ($p=0.542$, modified robust Brown-Forsythe Levene-type test) before the MW-U test. All performed tests were two-sided. A supplementary methods checklist is available.

Supplementary Material

Refer to Web version on PubMed Central for supplementary material.

ACKNOWLEDGEMENTS

We thank Marlies Kaiser, Ellen Stier, Sebastiano Bellanca, Philip Hasel and Marianna Karageorgi for technical assistance, Niklas Neef and Martin Lukat for building the treadmill and headplates, and Rebecca Jordan for help with behavioral experiments. We also thank David Gire, Rafi Haddad, Leslie Kay, and Dima Rinberg for discussion, and Troy Margrie, Zoltan Nusser and Dennis Burdakov for comments on the manuscript. This work was supported by the Excellence Cluster Cell Networks (postdoctoral fellowship to M.K.), the Max-Planck-Society, DFG (SPP1392), the MRC (MC_UP_1202/5), and the Alexander-von-Humboldt foundation (postdoctoral fellowship to I.F.). A.T.S. is a member of the Interdisciplinary Center for Neuroscience and the Bernstein-Center.

Europe PMC Funders Author Manuscripts

REFERENCES

1. Haider B, Häusser M, Carandini M. Nature. 2013; 493:97–100. [PubMed: 23172139]
2. Kato HK, Chu MW, Isaacson JS, Komiyama T. Neuron. 2012; 76:962–75. [PubMed: 23217744]
3. Gschwend O, Beroud J, Carleton A. PLoS One. 2012; 7:e30155. [PubMed: 22272291]
4. Shusterman R, Smear MC, Koulakov A, Rinberg D. Nat. Neurosci. 2011; 14:1039–44.
5. Cury KM, Uchida N. Neuron. 2010; 68:570–85. [PubMed: 21040855]
6. Fuentes R, Aguilar MI, Aylwin ML, Maldonado PE. J. Neurophysiol. 2008; 100:422–30. [PubMed: 18497360]
7. Kay L, Laurent G. Nat. Neurosci. 1999; 2:1003–1009. [PubMed: 10526340]
8. Rinberg D, Koulakov A, Gelperin A. J. Neurosci. 2006; 26:8857–65. [PubMed: 16928875]
9. Doucette W, Restrepo D. PLoS Biol. 2008; 6:e258. [PubMed: 18959481]
10. Blauvelt DG, Sato TF, Wienisch M, Knöpfel T, Murthy VN. Front. Neural Circuits. 2013; 7:46. [PubMed: 23543674]
11. Wachowiak M, et al. J. Neurosci. 2013; 33:5285–300. [PubMed: 23516293]
12. Davison IG, Katz LC. J. Neurosci. 2007; 27:2091–101. [PubMed: 17314304]
13. Shoham S, O'Connor DH, Segev R. J. Comp. Physiol. A. Neuroethol. Sens. Neural. Behav. Physiol. 2006; 192:777–84. [PubMed: 16550391]
14. Margrie TW, Brecht M, Sakmann B. Pflugers Arch. 2002; 444:491–8. [PubMed: 12136268]
15. Wohrer A, Humphries MD, Machens CK. Prog. Neurobiol. 2013; 103:156–93.
16. Pager J. Brain Res. 1983; 289:87–98. [PubMed: 6661658]
17. Bhalla US, Bower JM. J. Comput. Neurosci. 1997; 4:221–256. [PubMed: 9257234]
18. Matsumoto H, Kashiwadani H, Nagao H, Aiba A, Mori K. J. Neurophysiol. 2009; 101:1890–900. [PubMed: 19164106]
19. Balu R, Pressler RT, Strowbridge BW. J. Neurosci. 2007; 27:5621–32. [PubMed: 17522307]
20. Dietz SB, Murthy VN. J. Physiol. 2005; 569:475–88. [PubMed: 16166156]
21. Fukunaga I, Berning M, Kollo M, Schmaltz A, Schaefer AT. Neuron. 2012; 75:320–9. [PubMed: 22841316]
22. Cazakoff BN, Lau BYB, Crump KL, Demmer HS, Shea SD. Nat. Neurosci. 2014; 17:569–76. [PubMed: 24584050]
23. Abbott LF, Varela J. a, Sen K, Nelson SB. Science. 1997; 275:220–4. [PubMed: 8985017]
24. Boegerhausen M, Suter P, Liu S-C. Neural Comput. 2003; 15:331–48. [PubMed: 12590810]
25. Cang J, Isaacson JS. J. Neurosci. 2003; 23:4108–16. [PubMed: 12764098]

Europe PMC Funders Author Manuscripts

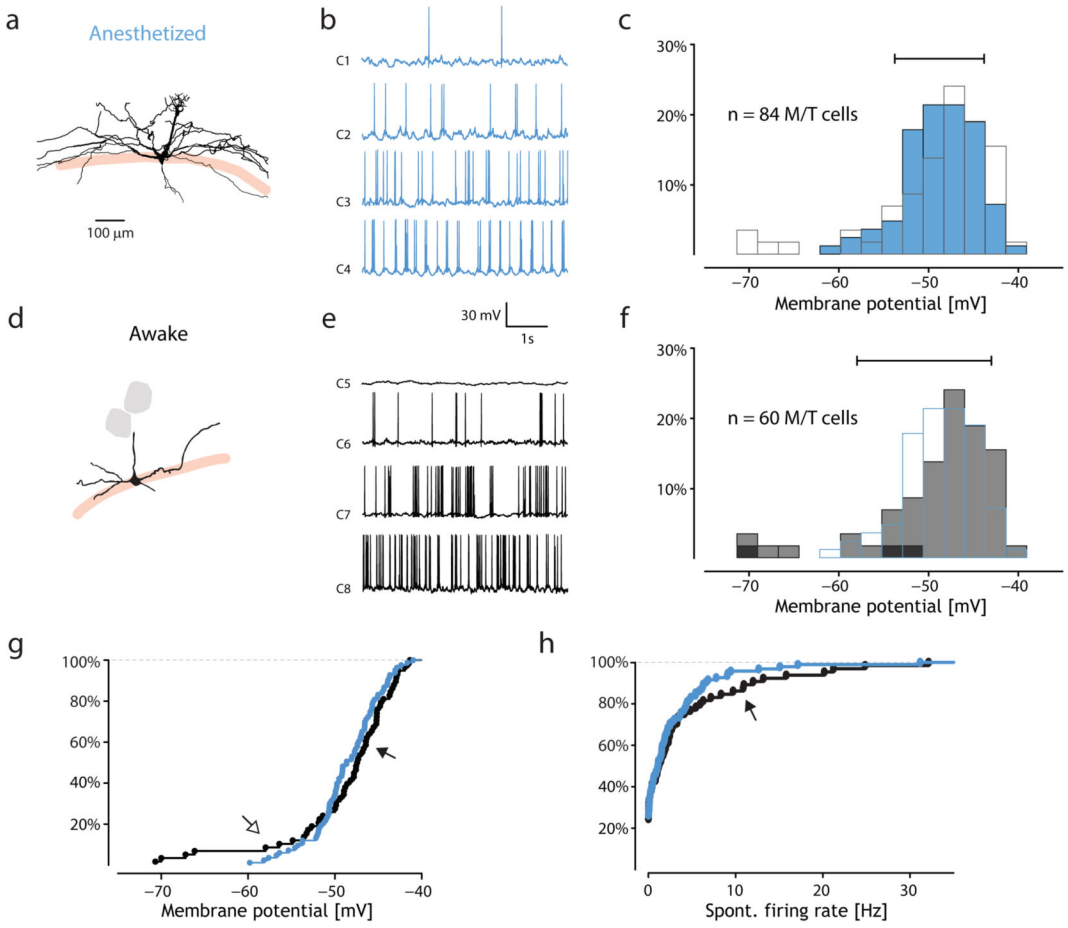

Figure 1. Baseline states of mitral/tufted cells in awake and anesthetized mice

Patch-clamp recordings from M/T cells of anesthetized (**a–c**) and awake mice (**d–f**). (**a, d**) Representative morphological reconstructions. (**b, e**) Four example M/TC recordings of baseline activity in each the awake (**e**, black) and the anesthetized (**b**, blue) preparation. (**c, f**) Distribution of baseline membrane potentials in M/T cells. Horizontal bars indicate the 10–90 percentile range. Dark grey bars in (**f**) represent recordings while the animal was performing an odor discrimination task (cf. Supplementary Fig. 1). Thin lines indicate the awake (c, black) and anthetized (f, blue) data for direct comparison. (**g**) Cumulative distribution of baseline membrane potential in M/T cells in awake (black, n = 60 M/TCs from 45 animals) and anesthetized (blue, n = 84 M/TCs from 51 animals) animals. Arrows indicate the increased number of both relatively hyperpolarized (open arrow) and relatively depolarized cells (black arrow) in recordings from awake compared to anesthetized mice. (**h**) Distribution of M/T cell firing rates of the same populations of cells as in (g) recorded in anesthetized (blue) or awake (black) mice. The black arrow indicates the significantly larger population of M/TCs in the awake animal with high baseline firing rate (firing rate > 10 Hz in 9/60 M/TCs in awake vs. 4/84 M/TCs in anesthetized).

Europe PMC Funders Author Manuscripts

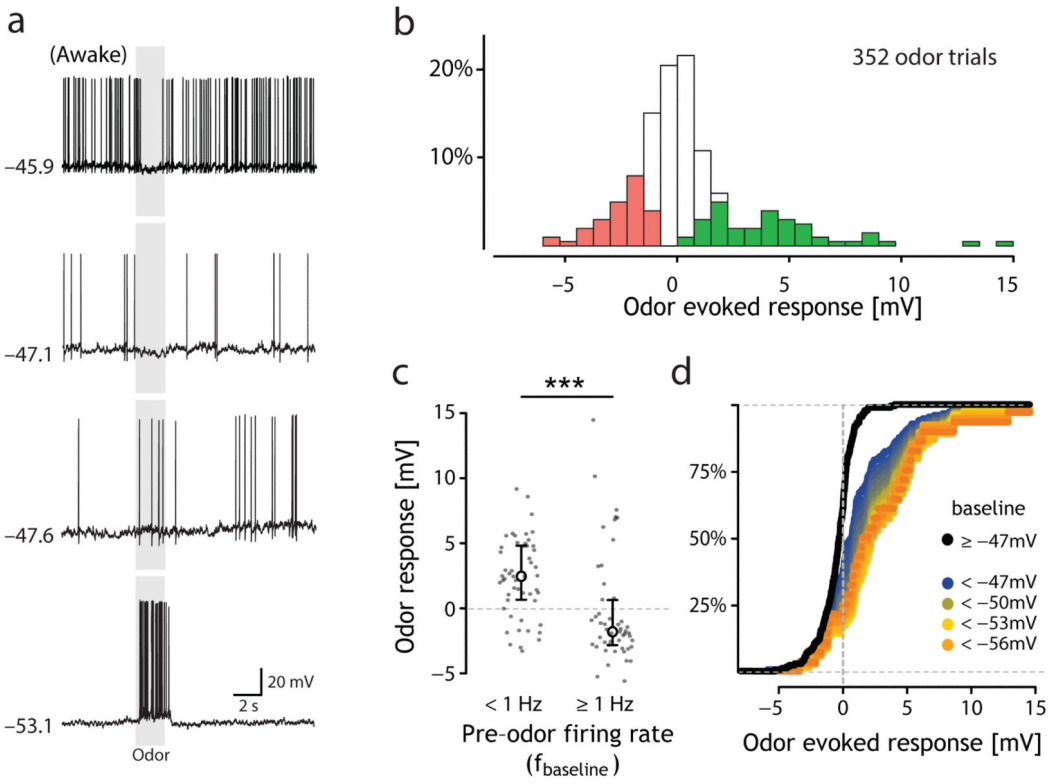

Figure 2. Odor evoked responses in mitral/tufted cells in awake mice are predicted by baseline activity

(**a**) Example traces of odor-evoked responses in four M/TCs recorded in awake mice. The respective average baseline membrane potential is indicated to the left of each trace (in mV). (**b**) Histogram of odor response amplitudes in M/TCs (n = 36 M/TCs from 36 animals, n = 352 odor responses). Significant ($p < 0.05$, see Online Methods) responses are displayed in green (n = 55 odor responses) and red (n = 47) for depolarizing and hyperpolarizing responses, respectively. (c) Relationship between recent firing behavior and odor evoked responses. (mean and 25th and 75th percentile, n = 52 odor-cell pairs from 15 M/T cells from 15 animals for $f_{baseline} < 1Hz$ and n = 50 from 13 M/T cells from 13 animals for $f_{baseline} \geq 1Hz$) (**d**) Cumulative distribution curves displaying the dependence of the odor response profiles of M/T cells on recent membrane potential (< −56 mV, n = 26 odor-cell pairs; < −53 mV, n = 38; < −50 mV, n = 46; < −47 mV, n = 53; ≥ −47 mV, n = 49). The most hyperpolarized cells (orange trace) respond preferentially with strong excitation, while depolarized cells (black trace) mainly show inhibition.